# BUTADIENE 1,4 POLYMERIZATION CATALYSIS

## II *. AN NMR STUDY OF THE STRUCTURE AND DYNAMICS OF BIS($\eta^3$-ALLYLNICKEL TRIFLUOROACETATE) AND ITS SIGNIFICANCE FOR THE MECHANISM OF THE POLYMERIZATION

R. WARIN **, M. JULÉMONT and Ph. TEYSSIÉ

*Laboratory of Macromolecular Chemistry and Organic Catalysis, University of Liège, Sart Tilman 4000 Liège (Belgium)*

(Received July 19th, 1979)

## Summary

$^1$H NMR study of the molecular dynamics of bis($\eta^3$-allylnickel trifluoroacetate) has revealed not only the important role of the metal—anion bond breaking in intra- and inter-molecular rearrangements but also the stability of the $\eta^3$-allyl coordination on the NMR time-scale. Implications for the mechanism of butadiene polymerization are discussed, and an interpretation of the control of the *cis—trans* isomer ratio is tentatively proposed.

## Introduction

Recent studies on stereospecific 1,4-polymerization of butadiene initiated by bis($\eta^3$-allylnickel(II) trifluoroacetate), (ANiTFA)$_2$, have indicated the selective formation of the so-called equibinary 1,4-polybutadiene (i.e. containing equal amounts of *cis* and *trans* 1,4-isomers) [1]. Moreover, it has been shown that the isomer distribution along the chain is determined to a large extent by the experimental conditions [2]. Unfortunately, while the structural characteristics of these polymers are well defined, the important questions of the *cis—trans* isomerism control mechanism and of the actual structure of the catalyst remain to be settled. We describe below the results of a detailed study of the catalytic system by $^1$H NMR spectroscopy, which allows observation of exchange reactions too fast to be followed by conventional kinetic methods.

---

* Part I, see ref. 24.
** To whom correspondance should be addressed.

## Results

### A. *Molecular dynamics of bis($\eta^3$-allylnickel trifluoroacetate) in chlorobenzene solution*

(1) At room temperature, as expected from similar studies on analogous $\eta^3$-allyl-transition metal complexes, the $^1$H NMR spectrum of (ANiTFA)$_2$ in chorobenzene appears as a AA'MM'X pattern characterized by two large coupling constants: $^3J_{AX} = {}^3J_{A'X} = 7.0$ Hz and $^3J_{MX} = {}^3J_{M'X} = 13.0$ Hz. Nevertheless, these values are lower than those expected for an $\eta^1$-allylic coordination ($^3J(H-H_{cis}) = 9-10$ Hz and $^3J(H-H_{trans}) = 17$ Hz), owing to a bond-order decrease induced by the $\eta^3$-coordination. The other coupling constants being very small ($\leqslant 0.5$ Hz), the spectrum displays an apparent A$_2$M$_2$X pattern, with $\delta_X$ 5.37 ppm, $\delta_A$ 2.69 ppm and $\delta_M$ 1.96 ppm (from TMS).

Like the *syn*-protons, the *anti*-nuclei are isochronous. This symmetry of the allyl group results from a mirror plane, orthogonal with it. Such a symmetry
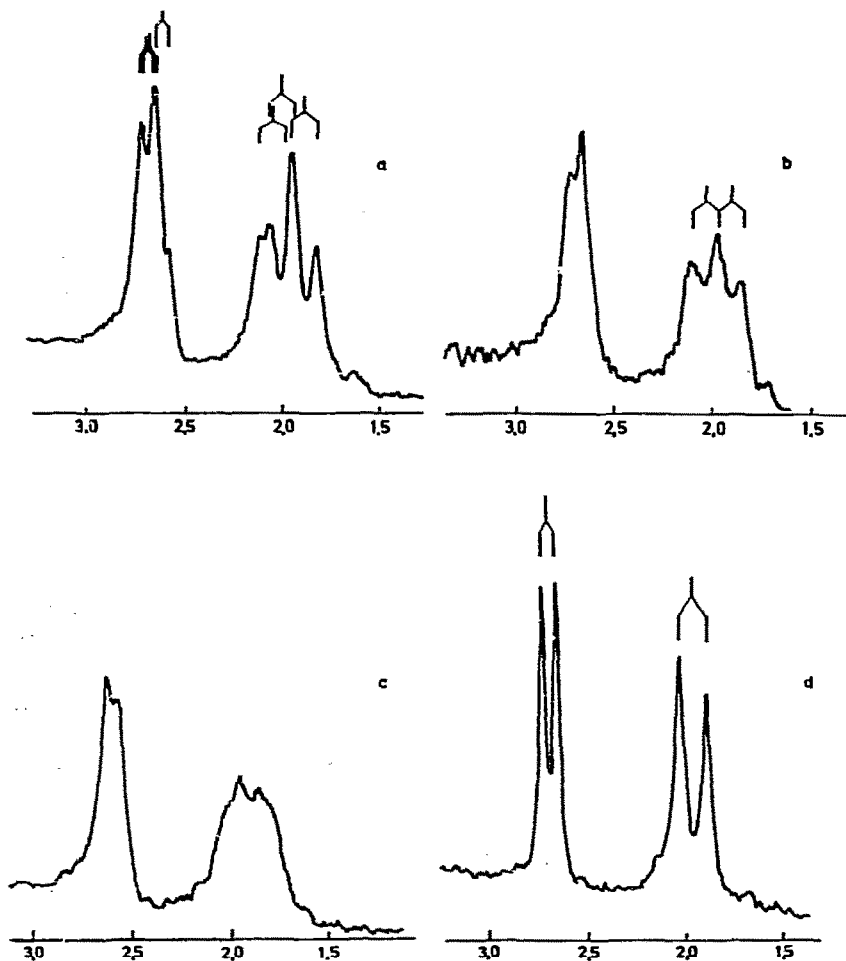


Fig. 1. 100 MHz spectra of bis($\eta^3$-allylnickel trifluoroacetate) (methylenic part) in chlorobenzene solution, as a function of temperature: (a) —75°C; (b) —45°C; (c) —35°C; (d) 0°C.

operation is also compatible with the proton noise-decoupled $^{13}C$ spectrum in benzene-$d_6$, i.e. a resonance at 112.5 ppm for the central carbon atom C(2) and another one for both the terminal carbon atoms C(1) and C(3) at 52.1 ppm (from TMS). The $sp^2$-hybridization of the allylic carbon nuclei is supported by the coupling constant values: $^1J$(C(2)—H) 158 Hz, $^1J$(C(1, 3)—H) 160 Hz and $^2J$(H$_{syn}$—H$_{anti}$) $\leqslant$ 0.5 Hz.

(2) When the temperature is lowered, the $^1H$ NMR spectrum is strongly modified: two overlapping AA′MM′X patterns are observed at −45°C and three spin systems are detected at −70°C (Fig. 1). Without sophisticated computer studies, a quantitative analysis is impossible, mainly due to the partial superposition of these coupled systems, whose populations are, moreover, temperature dependent. Consequently, the measurement of the coalescence temperatures ($T_c$) are very difficult, the more so as the signals undergo a weak temperature shift [3]. However, the $T_c$ values for the anti-protons were estimated as being at −40 and −55°C for the two and three spins systems, respectively. It must be stressed that warming the mixture above room temperature has never led to observation of coalescence of syn- and anti-resonances (AX$_4$ pattern) (resulting from the well-known $\eta^3 \to \eta^1 \to \eta^3$-allyl rearrangement [4]) before decomposition of the complex, in contrast to the behaviour of the corresponding Zr complexes [5].

These observations are consistent with the existence of two kinds of binuclear sandwich complexes in equilibrium (Fig. 2) very similar to those observed in the case of palladium [6—10]: (a) an asymmetric species (A) having a plane of symmetry bisecting the Ni—Ni axis and orthogonal with the allyl ligands; and (b) a symmetric species (S) having yet another plane of symmetry, perpendicular to the Ni—Ni axis and bisecting the sandwich (the corresponding head-to-head isomer is obviously sterically forbidden [7]).
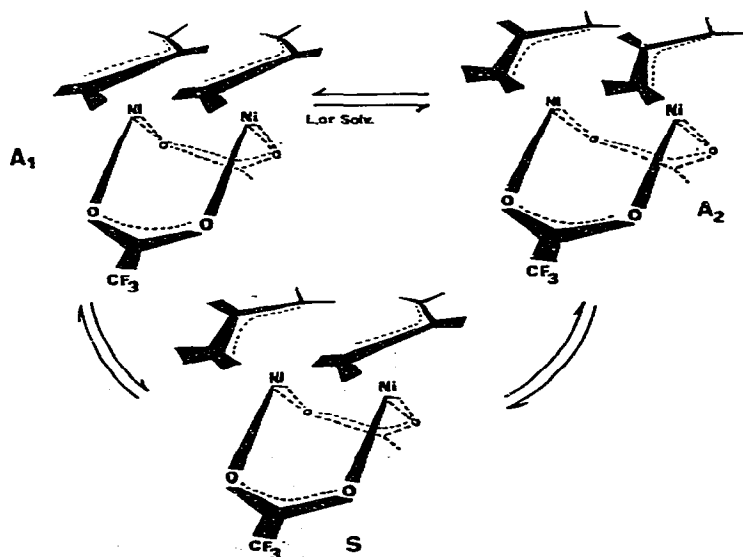


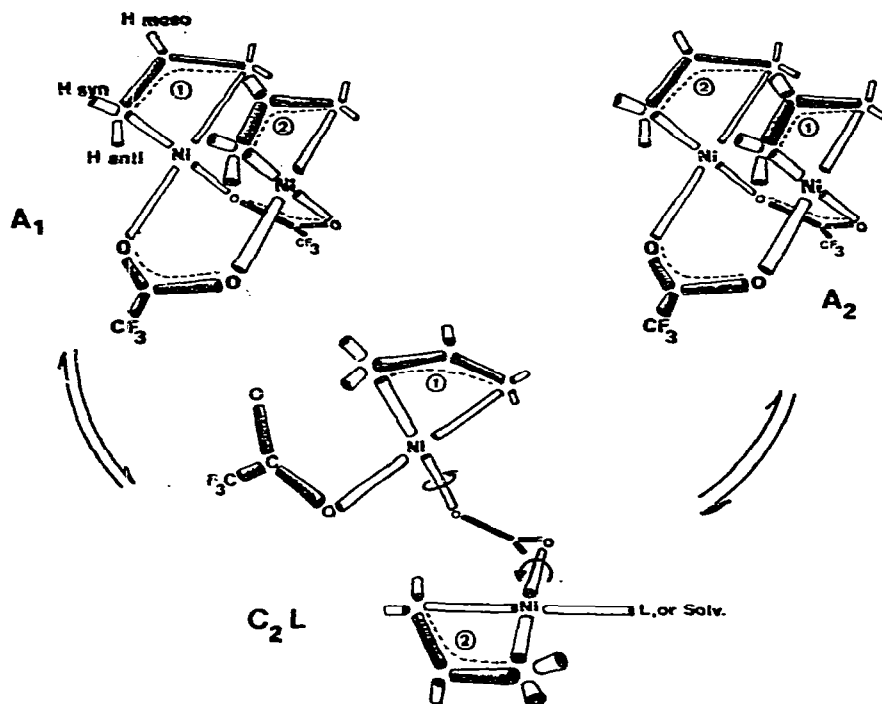Fig. 2. Diastomeric species of bis($\eta^3$-allylnickel trifluoroacetate).

Fig. 3. Interchange of enantiotopic allyl ligands without rupture of the *trihapto*-coordination.

Both $\eta^3$-allyl— or trifluoroacetate—metal bond cleavages could generate the observed dynamic exchanges. However, the $\eta^3$-allylic structure is too stable to allow fast rearrangements (no $AX_4$ pattern), especially at low temperature, and so only metal-anion exchanges can explain the temperature-dependent behaviour of $(ANiTFA)_2$.

We now reconsider all the exchanges detected on our NMR spectra.

(a) when the temperature is raised from —80 to —55°C, the first collapse observed involves one of the enantiotopic asymmetric isomers signals ($A_1 \rightleftharpoons A_2$ exchange on Fig. 3). In fact, this first exchange has been observed only with chlorobenzene solutions; in all the other solvents used it is still too fast even at —80°C [3]. Thus a solvent-assisted dissociative process must be considered: a mechanism involving dissociation via only one nickel—oxygen bond cleavage fits this requirement well. The $(Ni—O—C—O)_2$ ring opening in complex $A_1$, followed first by a rotation of one moiety with respect to the other one and then by formation of a new nickel—oxygen bond to close the bis-$\mu$ structure again, yields the other asymmetric species $A_2$. Accordingly, the complex always remains in a dimeric form. We do think that the inversion of the boat conformation of the $(Ni—OCO)_2$ ring, as previously proposed in analogous studies [8,9], would not be so sensitive to the nature of the solvent as the mechanism presented above.

(b) The second rate process appearing as the temperature is increased involves exchange of the symmetric (S) and asymmetric (A) diastereomers:

$A_{1, 2} \rightleftharpoons S$ (see Fig. 2). Such an interchange needs two Ni—O cleavages, either by means of an $(ANiTFA)_2 \rightleftharpoons 2 \, (ANiTFA)$ dissociative process or by intermolecular rearrangment (an intramolecular process being impossible without a coordination sphere rearrangement); both these mechanisms would be very sensitive to the nature of the solvent [3] because they involve solvent-assisted dissociations.

The $A_{1, 2} \rightleftharpoons S$ exchange most probably does involve a associative interaction of two binuclear entities $(ANiTFA)_2$ (possibly through the coordination vacancies temporarily liberated in equilibrium $A_1 \rightleftharpoons A_2$). Unfortunately, the bimolecular character of this exchange could not be fully confirmed experimentally owing to the limited complex solubility (ca. $3 \times 10^{-1} \, M$) and the difficulties in determining precisely the coalescence temperatures.

In principle, a completely dissociative mechanism via 2-bridges cleavage could be invoked also. This seems highly unlikely for various reasons: viz., it would imply an equally easy exchange of the three types of allyl groups with consequent very close coalescence temperatures, would give rise to very unlikely monomeric species (in terms of structure and statistical energy), and would conflict with some of the characteristics of the catalytic butadiene polymerization.

Whatever the detailed mechanism, the most important result of the above analysis is the evidence for the stability of the $\eta^3$-allylic coordination, implying that the equivalence process occurring on the NMR time-scale are due to intra- or inter-molecular Ni—O bond cleavages to the exclusion of any $\eta^1$-allylic pathway.

### B. Molecular dynamics of bis($\eta^3$-allylnickel trifluoroacetate) in butadiene solution

Similar experiments were carried out in liquid butadiene-$d_6$ as solvent. Under these conditions, an equilibrium between symmetric and asymmetric binuclear species is also observed, which must again be ascribed to the ready dissociation of the Ni—O bond. Consequently, the decrease of $T_c$ (syn-protons) from $-45°C$ in chlorobenzene to $-65°C$ in butadiene (the line separation being virtually identical: 7 Hz) may be considered as an indirect proof for the highly probable interaction between butadiene and the nickel atom *. Indeed, competition between butadiene and the trifluoroacetate anion for the same coordination site must increase the probability of cleaving Ni—O bonds, and consequently the rate of exchange between symmetric and asymmetric species. In such a solvent, the two types of allyl groups in the asymmetric binuclear complex cannot be observed even at temperatures as low as $-80°C$ (close to the freezing point).

It should be emphasized that even at $-40°C$, butadiene monomer molecules are inserted between the allyl ligand and the nickel atom. In non-deuterated butadiene as solvent the increasing intensity of the polybutadiene methylene proton signal ($\delta_H$ 2.07 ppm from TMS) and the decreasing intensity of the ini-

---

* Butadiene—nickel coordination complexes have not been identified experimentally in the NMR spectra. Populations and relaxation times of free and bounded butadiene molecules being very different, the weighted average value of the shift under fast exchange conditions is very close to the shift of the free butadiene molecule.
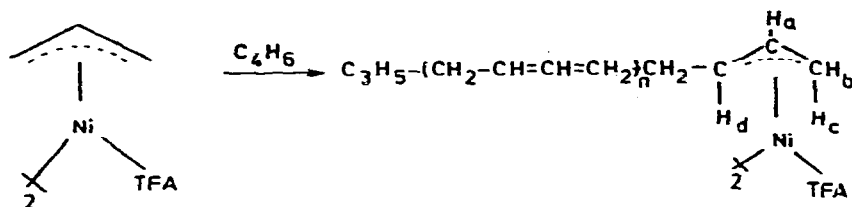
Fig. 4. Formation of growing chains ($\eta^3$-polybutadienylnickel trifluoroacetate).

tial allyl group proton resonances indicate the progressive conversion of the $\eta^3$-allylnickel into $\eta^3$-polybutadienylnickel complexes (Fig. 4).

We note that the usually good resolution of the spectra is decreased during the polymerization process and restored when it is stopped by cooling [11]. This observation is probably to be associated to an exchange between diamagnetic ($C_2$) and paramagnetic species (e.g. $C_2^*B$ with one Ni atom in a tetrahedral geometry). Due to the short lifetime and the low concentration of paramagnetic species, only a linewidth increase (and not shift change) is observed. On the other hand, a decrease of this linewidth upon lowering the temperature must be connected with a fall in the probability of forming the paramagnetic species.

Finally, even under these favorable experimental conditions, no $\eta^3$-allylic *anti—syn* isomerization is observed. Moreover, as previously reported [11], only *syn*-$\eta^3$-polybutadienyl complexes are observed, as demonstrated by the value of the $^3J_{a-d}$ (13 Hz), although both *cis* and/or *trans* olefins can be formed under these conditions; this is in apparent contradiction with the mechanisms proposed by Otsuka [12] and by Dolgoplosk [13—15].

## Discussion

### (a) Importance of μ-ligands exchange

This cleavage of nickel—μ ligand bonds, as detected by the NMR time-dependent studies reported hereabove, is undoubtedly of significance for the overall mechanism of butadiene 1,4-polymerization, and especially to its statistics of propagation. As demonstrated previously, the nature of the μ-ligand does closely control the rate of the polymerization [16], which is greatly enhanced (more than $10^3$ times) by increasing the electron-withdrawing character of the counter-anion.

It is known that bidentate μ-carboxylates are more easily monocoordinated to the nickel atoms as their basicity decreases (e.g. from acetate and chloroacetates to trifluoroacetate [17]). The resulting vacant coordination positions can then be occupied by other ligands, such as reactive butadiene molecules (see Fig. 3). The greater reactivity of (ANiTFA)$_2$ could be related to this fact, but also and, perhaps more importantly, be due to the fact that electron-withdrawing effect leads to easier conversion of the $\eta^3$-allyl into $\eta^1$-allyl groups.

The solvent effect [2] which determines the resulting polydiene microstructure can also be correlated with the solvation of the carboxyl groups, which create a solvent cage around the complex [3]. This could result in stabilization

of the species $C_2L$ (Fig. 3), the formation of which precedes the equibinary polymerization.

### (b) $\eta^3 \to \eta^1$ isomerization process and butadiene insertion

Within the frame of the *cis*-rearrangement scheme * proposed by Cossee [18] and Arlman [19], the insertion step in the growing chain propagation involves a preliminary $\eta^3 \to \eta^1$ isomerization process; this liberates a vacancy which is immediately occupied by the two bonds of a monomer molecule. Prior monomer coordination to the open form of the complex resulting from the Ni—O bond cleavage (see above) is probably needed for this higher activation energy step ($\eta^3 \to \eta^1$), in agreement with the kinetic equation for the whole propagation process [20]. Following a coordination sphere electronic rearrangement the butadiene is than rapidly inserted between the growing chain and the metal.

Unfortunately, the very low concentration of observable $\eta^1$-allyl active species associated with their short life-times in the NMR time scale prevents their detection in the spectra. On the basis of the spectroscopic data and evidence from the polymerization studies, we are now able to make a tentative explanation of the *cis—trans* isomer control and of the overall propagation mechanism.

### (c) The cis—trans isomer control mechanism and anti—syn $\eta^3$-allylnickel reactivity

The slowness of butadiene polymerization initiated by $(ANiTFA)_2$ as well as the high stability of the $\eta^3$-allylic coordination demonstrated by the NMR experiments lead us to assume that after insertion the $\eta^1$-polybutadienylnickel complex returns quickly to the $\eta^3$-species, the "sleeping" form of the catalyst. In this step, an *anti*-configuration will arise from the insertion of a bidentate *s-cis*-coordinated butadiene molecule while a *syn*-configuration will come from a *s-trans*-monomer molecule [23].
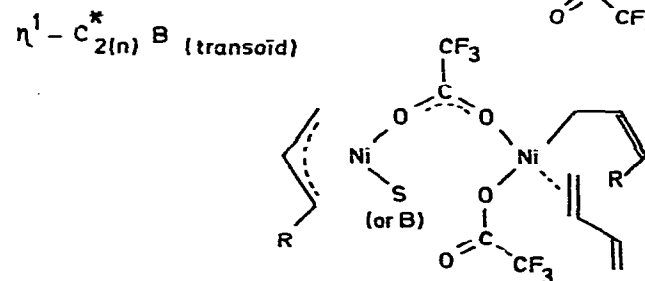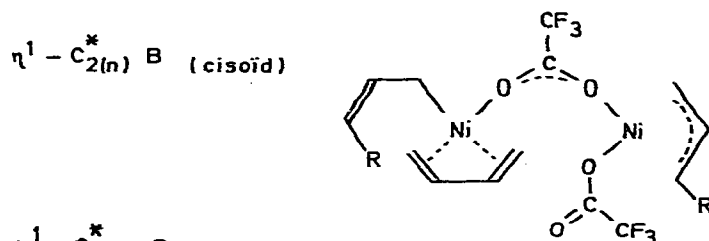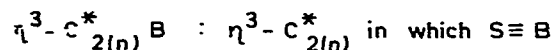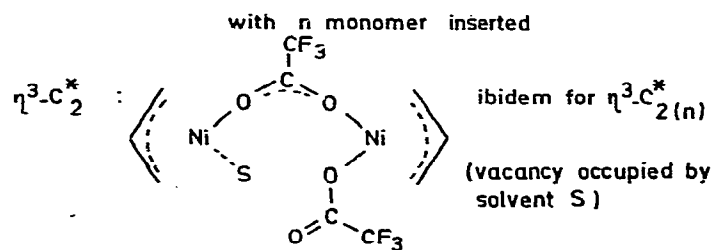
Provided any *anti—syn* isomerization does not occur on the time scale of the insertion, the two different coordination modes offer an interpretation of the mechanism controlling the *cis—trans* isomerism, since for the next insertion step the initial conversion of the growing chain into the $\eta^1$-structure will liberate a *cis* or a *trans* penultimate unit. The absence of *anti—syn* isomerization is confirmed not only by the independence of the anti and syn protons in the NMR spectra but also by the specific formation of the equibinary polybutadiene in a large range of initial monomer versus catalyst molar ratio. Conversely, a hypothetical variation of the microstructure versus this ratio would have suggested a competition between the kinetically concentration and temperature dependent $\eta^3 \to \eta^1$ isomerization and an effective *anti—syn* isomerization. Consequently, it is really a geometrical factor, viz. the conformation of the coordinated butadiene molecule, which finally controls the *cis—trans* ratio.

Since only *syn*-$\eta^3$-polybutadienylnickel growing chains are observed, *anti* species must be assumed to be characterized by a much lower free activation

---

* This scheme remains the most probable in the presence of $(ANiTFA)_2$ since, in the dissymmetric bis($\eta^3$-crotylnickel trifluoroacetate), the less substituted allylic carbon atoms is the most strongly $\sigma$ bonded to the metal, in contrast with the features needed to interpret the butadiene polymerization in terms of an allylic transposition mechanism [21,22].

energy for $\eta^3 \to \eta^1$ transition ($\Delta G^{\#}_{\eta^3 \to \eta^1}$) than for the $\eta^3 \to \eta^1$ *syn*-process. Accordingly, the *anti* isomers would display such a higher reactivity that its very short lifetime (and consequently its concentration) would not permit its detection in the NMR spectra. This also means that when a *syn*-isomer is obtained it will remain for a longer time in this "hypersleeping" configuration than the *anti*-isomer.

These two different free activation energies determine the different initiation rates by $\eta^3$-allyl or $\eta^3$-crotyl catalysts which are always in the *syn* configuration [11]. The initiation step of butadiene polymerization by bis($\eta^3$-crotylnickel trifluoroacetate) proceeds from the *syn*-configuration, the $\Delta G^{\#}_{\eta^3 \to \eta^1}$ of which should be higher than $\Delta G^{\#}_{\eta^3 \to \eta^1}$ of (ANiTFA)$_2$, and this explains its lower initiation rate.

$\eta^3 - C_2$ :    bis($\eta^3$-allyl nickel trifluoroacetate)

$\eta^3 - C_{2(n)}$ :    bis($\eta^3$- polybutadienylnickel trifluoroacetate)



with n monomer inserted

$\eta^3 - C^*_2$ :    ibidem for $\eta^3 - C^*_{2(n)}$

(vacancy occupied by solvent S )

$\eta^3 - C^*_{2(n)}$ B :    $\eta^3 - C^*_{2(n)}$ in which S ≡ B

$\eta^1 - C^*_{2(n)}$ B  (cisoïd)



$\eta^1 - C^*_{2(n)}$ B  (transoïd)



$\eta^3 - C_{2(anti)(n)}$   and   $\eta^3 - C_{2(syn)(n)}$ representing respectively
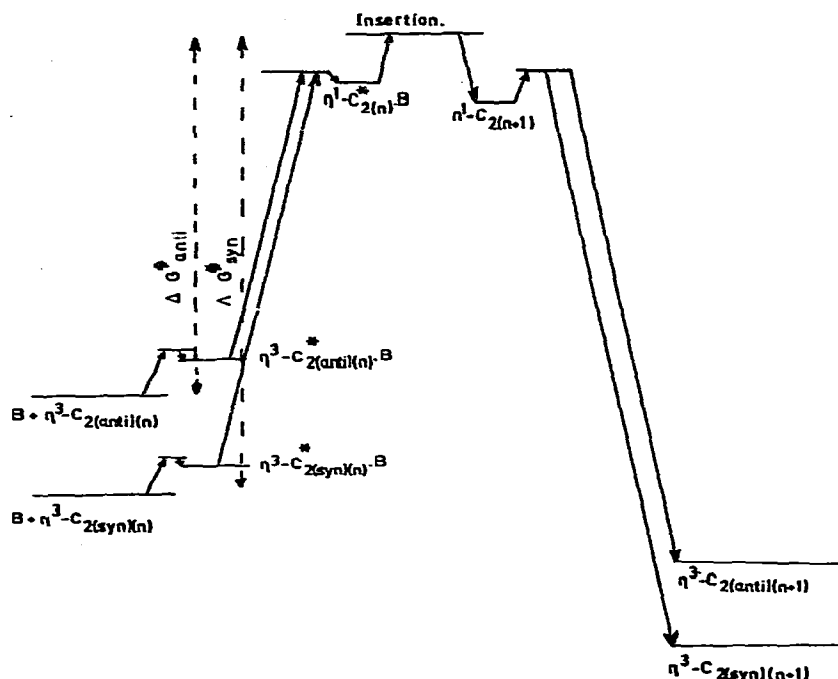
anti - and syn - growing chains .

Fig. 5. (a) Notations and structure; (b) Tentative energy diagram related to insertion process.

## (d) Tentative kinetic scheme for the overall process

While the isomerism of the inserted 1,4-units is determined by the coordination mode of the monomer, the polymerization rate depends on the $\eta^3 \to \eta^1$ allylic isomerization regarded as the rate-determining step of the overall process. This is not in contradiction with the high stability of the $\eta^3$-allyl coordination detected from the NMR studies since the polymerization time scale is much longer (around 10 insertions per hour at room temperature) than the NMR time scale (20 exchanges per sec at $-50°$C).

The coordination of the monomer, promoting the cleavage of one Ni—O bond, most probably stabilizes the resulting dissociated species of the binuclear complex $C_2^*$. If $C_{2(n)}$ stands for a bis($\eta^3$-polybutadienylnickel) complex obtained after $n$ inserted butadiene (B) units, the kinetic scheme (Scheme 1) illustrated in Fig. 5, may be tentatively proposed to interpret the overall propagation process (see also the appendix).

fast: $\eta^3$—$C_{2(n)} \underset{k_{-1}}{\overset{k_1}{\rightleftharpoons}} \eta^3$—$C_{2(n)}^*$ without B;

with $K_1 = \dfrac{k_1}{k_{-1}} = \dfrac{[\eta^3-C_{2(n)}^*]}{[\eta^3-C_{2(n)}]}$ (1)

fast: $\eta^3$—$C_{2(n)} + B \underset{k_{-2}}{\overset{k_2}{\rightleftharpoons}} \eta^3$—$C_{2(n)}^* B$ in the presence of B;

with $K_2 = \dfrac{k_2}{k_{-2}} = \dfrac{[\eta^3-C_{2(n)}^* B]}{[\eta^3-C_{2(n)}][B]}$ (2)

$$\text{slow:} \quad \eta^3\text{—}C^*_{2(n)}B \underset{k_{-3}}{\overset{k_3}{\rightleftharpoons}} \eta^1\text{—}C^*_{2(n)}B \tag{3}$$

$$\eta^1\text{—}C^*_{2(n)}B \overset{k_4}{\rightarrow} \eta^1\text{—}C_{2(n+1)} \tag{4}$$

$$\eta^1\text{—}C_{2(n+1)} \overset{k_5}{\rightarrow} \eta^3\text{—}C_{2(n+1)} \tag{5}$$

Equations 3 and 4 result in a stationary system; the values of both $K_1$ and $K_2$ are very low.

This scheme may explain the following phenomena: (1) if a strong ligand (L) competes with B for nickel, s-*trans*-coordinated butadiene molecules (on $C_2L$ or CL species, depending on the amount and the basicity of L) will lead to a *trans*-polybutadiene formation through only *syn*-$\eta^3$-polybutadienylnickel intermediates.

(2) Upon lowering the temperature, the *cis*-content in the polymer is enhanced. Owing to the difference between the respective values of $\Delta G^{\#}_{\eta^3 \rightarrow \eta^1}$, the reactivity of *anti*-$\eta^3$-species must be increased relative to that of the *syn*-$\eta^3$-species, so that *cis*-polymerization is kinetically favoured under these conditions.

All these features will be considered in detail in further publications in connection with the experimental characteristics of butadiene equibinary 1,4-polymerization.

*(e) Comparison with analogous palladium complexes*

Probably because of their identical basic structural characteristics, $\eta^3$-allylnickel complexes exhibit dynamical behaviour quite similar to that described for analogous palladium complexes. As for palladium complexes [8], two equilibria between different binuclear isomers were detected; moreover in both palladium and nickel complexes no coalescence of the *syn—anti* protons resonances is observed even at room temperature. However, in the presence of butadiene *anti-syn* isomerization is observed not only for the protons in the initial species but also for the substituent in the addition product, in the case of palladium complexes [21] but not of nickel complexes. This difference is to be associated with: (1) the higher tendancy of $\eta^3$-allylpalladium complexes to isomerize to $\eta^1$-species compared with the homologous nickel complexes [25] and (2) the higher probability of insertion of the coordinated butadiene molecule into the $\eta^1$-allylnickel complex than into the palladium species. Accordingly, instead of promoting the *syn—anti* isomerization as a temporary ligand, the butadiene coordinated to the nickel atom is quickly inserted between the metal and the $\eta^1$-allyl group, in contrast to the behaviour of analogous palladium complexes.

In addition, because of steric and electronic differences there are marked differences in mechanism: while the palladium-catalyzed 1,2-addition reaction is well explained in terms of allylic transposition [21], such an outer-sphere pericyclic rearrangement does not fit the characteristics of the 1,4-diene polymerization (see below); moreover it gives no interpretation of the very efficient *cis—trans* isomeric control that we have achieved with nickel initiators. A more detailed discussion of these mechanistic aspects will be published in the future.

## Conclusions

The conclusions reached in the present study can be expressed as a list of experimental facts and then as a list of mechanistic deductions.

### A. Experimental conclusions from the NMR study
The $\eta^3$-allyl coordination is very stable on the time scale involved.

The dynamics of $(ANiTFA)_2$ are due essentially to two types of exchange between 3 different species (1 symmetrical and 2 asymmetrical), both occurring through nickel—oxygen bond cleavage.

The faster exchange involves an intramolecular process requiring only partial opening of the complex, while the slower one is most probably a bimolecular reaction, although it is not possible to exclude completely a total dissociation into mononuclear entities.

These bond openings are clearly solvent-assisted; the butadiene monomer is particularly efficient in this respect.

### B. Mechanistic implications of the results
The polymerization reaction initiated by this complex involves a monomer cis-insertion propagation mechanism, which in turn implies as a prerequisite the $\eta^3$-allyl → $\eta^1$-allyl isomerization of the active end of the growing-chain; this isomerization is the rate-determining step in the overall process, and after every insertion the active complex reverts to the $\eta^3$-allyl type of coordination.

Under the conditions used for the spectroscopic investigation and the polymerizations there is no anti—syn isomerization.

The rate of monomer insertion depends on the configuration of the last unit inserted: the $\Delta G^{\neq}$ of the anti-growing chains is markedly lower than that of the syn-species. Thus detection of the anti-species has not been possible.

The microstructure of the resulting polymer is strongly determined by the mode of coordination of butadiene (mono- or bi-dentate), i.e. by the numerous structural kinetic and thermodynamic factors which control this coordination.

The equibinary 1,4-polymerization cannot be explained by the allylic transposition mechanism invoked in the case of allylpalladium initiators.

All these conclusions will be further applied to various aspects of butadiene selective 1,4-polymerization, to be reported elsewhere.

## Experimental

The synthesis of bis($\eta^3$-allylnickel trifluoroacetate) involved an improvement of the method described by Dawans et al. [16]. Solid di-1,5-cyclooctadiene-nickel(0) (carefully recrystallized) was dissolved in a benzene solution of allyl trifluoroacetate for half an hour (molar ratio of reactants: 1/1.05) under argon at room temperature. The complex was isolated by lyophilisation from the reaction medium ($10^{-2}$ mmHg at room temperature for 3 h).

The spectroscopic studies were performed under argon using $3 \times 10^{-1}$ $M$ solution containing tetramethylsilane as internal standard, in dried and oxygen-free tubes. The measurements were carried out with a HA 100 VARIAN spectrometer for $^1$H NMR spectra and a HFX 90 BRUCKER spectrometer for $^{13}$C NMR analysis.

424

## Appendix: Kinetic aspects

As shown above, the $\eta^1$-allyl-growing chain probably reverts to the $\eta^3$-state after each insertion. Consequently, the polymerization rate, equal to the rate of the $\eta^3 \rightarrow \eta^1$ isomerization, i.e. the slowest step of the overall process, will be related to the isomerism of the inserted monomeric units.

However, under the conditions of the 1,4-equibinary polymerization, each nickel center promotes the formation of an equal amount of cis- and trans-isomers and so will display the same average activity. Accordingly, in the following development connected with the tentative mechanism and giving account of the observed kinetic law (first order in both nickel and butadiene concentrations [20]), each catalytic center will be represented by $\eta^3$-$C_{2(n)}^*B$, irrespective of whether these is syn- or anti-isomerism of the allyl ligand.

$$-\frac{d[\eta^3 - C_{2(n)}^*B]}{dt} = k_3[\eta^3 - C_{2(n)}^*B] - k_{-3}[\eta^1 - C_{2(n)}^*B] \tag{6}$$

If we accept the approximation of a stationary state, we have:

$$\frac{d[\eta^1 - C_{2(n)}^*B]}{dt} = k_3[\eta^3 - C_{2(n)}^*B] - k_{-3}[\eta^1 - C_{2(n)}^*B] - k_4[\eta^1 - C_{2(n)}^*B] = 0$$

$$= k_3[\eta^3 - C_{2(n)}^*B] - (k_{-3} + k_4)[\eta^1 - C_{2(n)}^*B] = 0$$

and $[\eta^1 - C_{2(n)}^*B] = \dfrac{k_3[\eta^3 - C_{2(n)}^*B]}{k_{-3} + k_4}$ \hfill (7)

with eq. 7, eq. 6 becomes:

$$\frac{-d[\eta^3 - C_{2(n)}^*B]}{dt} = k_3[\eta^3 - C_{2(n)}^*B] - k_{-3}k_3 \frac{[\eta^3 - C_{2(n)}^*B]}{k_{-3} + k_4}$$

$$= \frac{k_3 k_4}{k_{-3} + k_4}[\eta^3 - C_{2(n)}^*B] . \tag{8}$$

From eq. 2: $[\eta^3 - C_{2(n)}^*B] = K_2[\eta^3 - C_{2(n)}^*][B]$

Eq. 8 $\rightarrow \dfrac{-d[\eta^3 - C_{2(n)}^*B]}{dt} = \dfrac{k_3 k_4}{k_{-3} + k_4} \cdot K_2[\eta^3 - C_{2(n)}^*][B]$

$$= \frac{k_3 k_4}{k_{-3} + k_4} \cdot K_1 K_2[\eta^3 - C_{2(n)}][B] = k_{exp.}[\eta^3 - C_{2(n)}][B]$$

# References

1 J.P. Durand and Ph. Teyssie, J. Polym. Sci., B6 (1968) 229.
2 Ph. Teyssie, M. Julemont, J.M. Thomassin, E. Walckiers and R. Warin, in J.C.W. Chien (Ed.), Coordination Polymerisation, Academic Press Inc., New York, 1975, p. 327; see also Ph. Teyssie, A. Devaux, P. Hadjiandreou, M. Julemont, J.M. Thomassin, E. Walckiers and R. Warin, The Control of Diolefins Selective Polymerization, in F. Ciardelli and R.W. Lenz (Eds.), Nato Advanced Study Institute on stereoregulars polymers, Plenum Press, London, in press.
3 M. Julemont, R. Warin, Ph. Teyssie, J. Molec. Catalysis, submitted.
4 e.g. J. Powell and B.L. Shaw, J. Chem. Soc. A, (1967) 1839.
5 J.K. Beconsall, B.E. Job and S. O'Brien, J. Chem. Soc. A, (1967) 423.
6 M.R. Churchill and R. Mason, Nature, 204 (1964) 777.
7 M.R. Churchill and R. Mason, Advan. Organometal. Chem., 5 (1967) 105.
8 J. Powell, J. Amer. Chem. Soc., 91 (1969) 4311.
9 P.W.N.M. Van Leeuwen and A.P. Praat, Rec. Trav. Chim. Pays-Bas, 89 (1970) 321.
10 P.W.N.M. Van Leeuwen, J. Lukas, A.P. Praat and M. Appelman, J. Organometal. Chem., 38 (1972) 199.
11 R. Warin, Ph. Teyssie, P. Bourdauducq and F. Dawans, J. Polym. Sci., Polym. Lett., 11 (1973) 177.
12 S. Otsuka and M. Kawakami, Kogyo Kagaky Zasshi, 68 (1965) 874.
13 B.A. Dolgoplosk et al., Dokl. Phys. Chem., 205 (1972) 602.
14 B.A. Dolgoplosk et al., Dokl. Akad. Nauk. SSSR, 173 (1967) 1087.
15 B.A. Dolgoplosk et al., J. Polym. Sci., A.1, 11 (1973) 2569.
16 F. Dawans and Ph. Teyssie, J. Polym. Sci., L. 7, (1969) 111.
17 R.P. Hughes, T. Jack and J. Powell, J. Organometal. Chem., 63 (1973) 451.
18 P. Cossee, J. Catal., 3 (1964) 80.
19 E.J. Arlman, J. Catal., 5 (1966) 178.
20 J.C. Marechal, F. Dawans and Ph. Teyssie, J. Polym. Sci., A, 8 (1970) 1993.
21 R.P. Hughes and J. Powell, J. Amer. Chem. Soc., 94 (1972) 7723.
22 A. Devaux and M. Julemont, unpublished results.
23 C.A. Tolman, J. Amer. Chem. Soc., 92 (1970) 6777.
24 M. Julemont, E. Walckiers, R. Warin and Ph. Teyssie, Makromol. Chem., 175 (1974) 1673.
25 P.M. Maitlis, The Organic Chemistry of Palladium, Vol. I Academic Press, New York, 1971, p. 225.